deg facets. The various stages in the fracture process can be seen in Fig. 7(*b*) which is of an area located behind the fracture surface. First, isolated fracturing of some of those cementite platelets oriented approximately parallel to the stress direction occurs. Fracturing of the platelets then continues across the pearlite colony with the fractures lining up approximately at 45 deg to the stress direction (arrow). The second step involves the growth of voids emanating from the separation of the two parts of the fractured platelet. These voids then grow through the pearlitic ferrite and link up to form a crack across the colony. This is followed by the joining of cracks from adjacent colonies to form a major crack. Finally, this major crack grows by the continuation of this ductile pearlite fracture mechanism along with cleavage of the pearlite. The electron fractograph, Fig. 7(*c*), shows the later stages of fracture which is a mixture of long parallel dimples (arrow) characteristic of the ductile pearlite fracture process described above, and pearlite cleavage.

The effects of a superposed hydrostatic pressure of 22.8 kbars on the fracture appearance in this material are shown in Fig. 8. At this pressure the fracture surface has converted to a flat planar shear type, Fig. 8(*a*). In the region of the fracture surface, it is no longer possible to readily resolve the microstructure optically except that it consists of a series of light and dark lands. There is no evidence of pearlite cleavage or voids and associated ductile fracturing of the pearlite as was evident at atmospheric pressure.

Behind the fracture surface, Fig. 8(*b*), it can be seen that the cementite oriented parallel to the tensile direction is extensively fractured; the fractures lining up approximately along the 45 deg plane (arrow). As also shown in Fig. 8(*b*), in those pearlite colonies not oriented parallel to the tensile direction, the cementite undergoes severe bending prior to extensive fragmentation as the fracture surface is approached. Although the cementite still extensively fractures under the superposed pressure of 22.8 kbars, the pressure has imparted considerable ductility to this brittle phase as evidenced by the bending.

The electron fractograph, Fig. 8(*c*), is effectively flat and featureless showing no evidence of dimples or cleavage.

b) *Annealed 0.40 pct C Material.* The fracture appearance in the annealed 0.40 pct C hypoeutectoid steel tested at atmospheric pressure is shown in Fig. 9. As seen in Fig. 9(*a*), the fracture profile is quite ductile in appearance. Many of the "hills" or "valleys" contain pearlite.

Behind the fracture surface, Fig. 9(*b*), it can be seen that the initial stage of fracture involves fracture of the pearlite. The observed fracture process of the pearlite was the same as that previously discussed in the 0.83 pct C material (platelet fracture and void growth in the pearlitic ferrite).

The final stage of fracture in this material involves the growth and link up of voids emanating from the fractured pearlite colonies. Such voids can be seen in Fig. 9(*a*).

An electron fractograph of a pearlite-ferrite interface is shown in Fig. 9(*c*). Long parallel dimples characteristic of the ductile fracture of pearlite are in evidence (arrow). Adjacent to the pearlite fracture are portions of large dimples corresponding to the void growth in the ferrite.

The appearance of a specimen of this material fractured at a pressure of 17.6 kbars is shown in Fig. 10. At this pressure, the fracture profile, Fig. 10(*a*), is of the planar shear type. There appears to be no

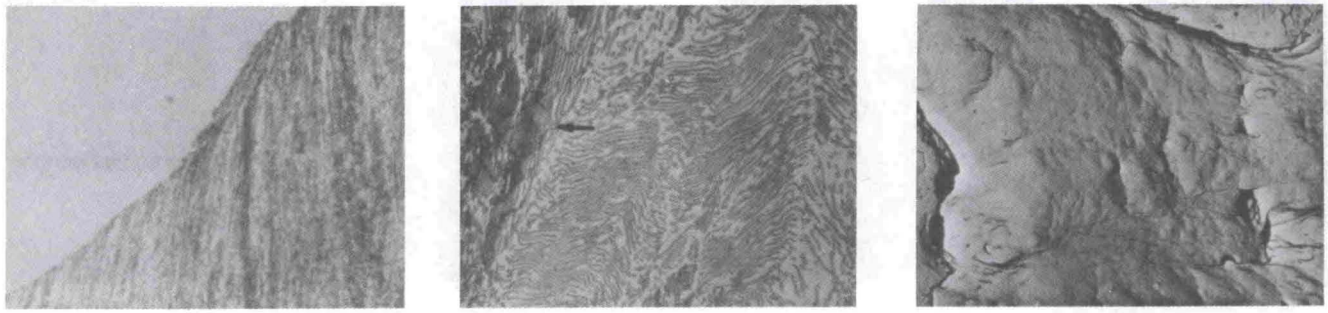

(*a*) (*b*) (*c*) ⊢5 μ⊣

Fig. 8—Fracture in annealed 0.83 pct C material at 22.8 kbars. (*a*) and (*b*) magnification 540 times.

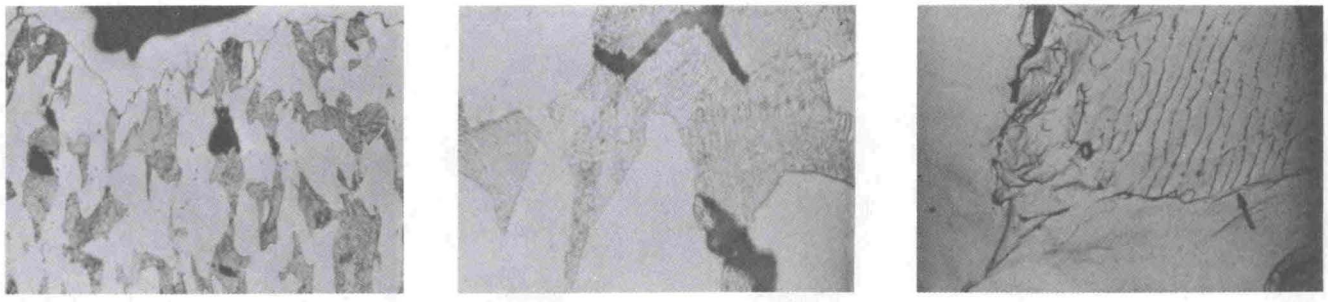

(*a*) (*b*) (*c*) ⊢5 μ⊣

Fig. 9—Fracture in annealed 0.40 pct C material at atmospheric pressure. (*a*) Magnification 106 times, (*b*) magnification 530 times.

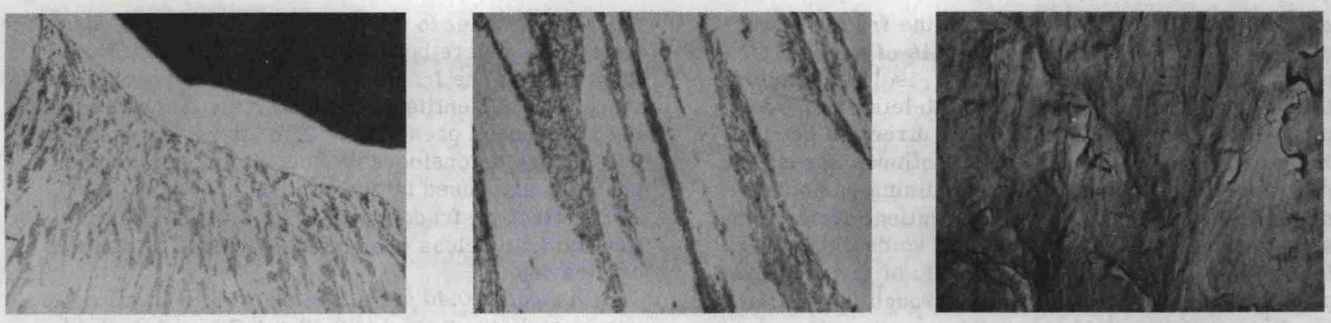

Fig. 10—Fracture in annealed 0.40 pct C material at 17.6 kbars. (*a*) Magnification 106 times, (*b*) magnification 530 times.

perturbations at the fracture surface associated with the pearlite as was the case at atmospheric pressure. As seen in Figs. 10(*a*) and (*b*) there are no voids or pearlite cracks in evidence. The cementite within the pearlite colonies, Fig. 10(*b*), is deformed and, near the fracture surface, is extensively fragmented as was the case in the eutectoid composition material. The electron fractograph, Fig. 10(*c*), reveals a fracture surface that is effectively featureless.

c) *Annealed 1.1 pct C Material.* Fracture in the annealed 1.1 pct C hypereutectoid steel at atmospheric pressure is shown in Fig. 11. As seen in Fig. 11(*a*), the fracture is generally intergranular and follows the cementite in the prior austenite boundaries. Behind the fracture surface, Fig. 6(*b*), it can be seen that the fracture occurs within the cementite at the austenite boundaries and not at the cementite-pearlite interface. Fracture of the cementite in the boundaries oriented parallel to the stress direction also occurs. However, these cracks are arrested (arrow) at the cementite-pearlite interface and do not enter into the fracture process. The electron fractograph for this material, Fig. 11(*c*), reveals a typical cleavage fracture appearance.

The effects of a pressure of 22.8 kbars on the fracture of this material are shown in Fig. 12. As seen in Fig. 12(*a*), the major portion of the fracture surface is of the planar shear type showing no discontinuities associated with the transverse or longitudinal cementite. It can also be seen that the hypereutectoid cementite is completely fragmented with the fragments (arrow) aligned parallel to the tensile stress direction. It can be seen in Fig. 12(*b*) that the fracture mode of the cementite has converted from cleavage to shear. There are no voids associated with the fragmented cementite which indicates that the pearlite may have been forced in between the separating fragments. Near the fracture surface, fracturing of the cementite within the pearlite was also observed. It appears that the hypereutectoid cementite no longer plays a role in the

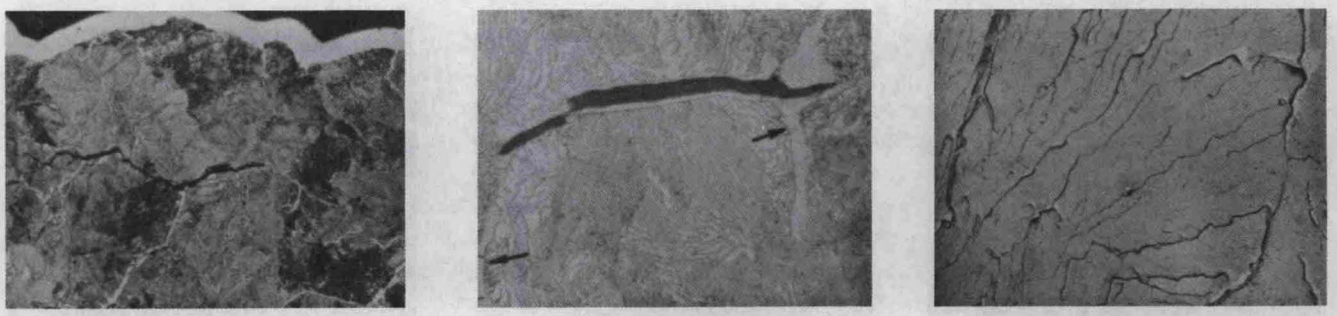

Fig. 11—Fracture in annealed 1.1 pct C material at atmospheric pressure. (*a*) Magnification 106 times, (*b*) magnification 530 times.

Fig. 12—Fracture in annealed 1.1 pct C material at 22.8 kbars. (*a*) and (*b*) magnification 530 times.